Al-Azhar University Civil Engineering Research Magazine (CERM)
Vol. (40) No. (3) July, 2018

Shear Behavior and Capacity of Composite Box Girder with Steel Corrugated Web

Prof. Dr. S. A. Hassanein, Assoc. Prof. Dr. E. S. Salem, Eng. A. M. Mohmoud
Civil Engineering Department, Faculty of Engineering Al-Azhar University

ملخص البحث

يقدم هذا البحث استنادا الي دراسة معملية ونمذجة عددية لسلوك القص للكمرات الصندوقية المركبة ذات الاعصاب المعدنية المموجة حيث تم تصنيع كمرتين ذات مقياس مناسب و تحمليهما باحمال استاتيكية حتي الانهيار وقياس الانفعلات والترخيم في الاماكن المحددة

وقد ابدي هذا النوع من الكمرات الصندوقية المركبة ذات الاعصاب المموجة سلوك اكثر ممطولية مقارنة بالكمرات التقليدية ذات العصب المعرج كما تم دراسة نموذج الانهيار للكمرات المختبرة في القص حيث تم ظهور منطقة قوي شد في الاعصاب المموجة بعد انبعاجها وهي المسؤلة عن مقاومة قوة القص بعد انبعاج الاعصاب. هذه القوة ترتكز في النهاية علي الشفة العلوية والسفلية للكمرة الصندوقية وعليه تبين تأثير جساءة هذة الشفات علي سلوك الكمرات الصندوقية في القص.

علاوة علي ذلك تم عمل نمذجة عددية للكمرات المختبرة واستنباط النتائج المطلوبة والتي جاءت متوافقة مع النتائج المعملية.

Abstract

Steel girders with corrugated web have been widely used in long span beams and bridges. In this paper, an experimental and finite element modeling are presented to investigate the behavior of composite box girder with steel corrugated webs under shear and bending moment. Two composite box girders with steel corrugated webs, were fabricated and tested. The first one was loaded in three points loading and the other was loaded in four points loading. Moreover, Finite element modeling for tested girders was conducted and the predicted results were compared with the experimental results. The tested girders behaved in elastic-plastic manner and the sudden failure of corrugated web in shear, typically observed in case of bare steel girder with corrugated web, was avoided.

Keywords: *corrugated web, composite box girder, shear strength, finite element analysis*

1. Introduction

Steel girder with corrugated web have widely used in long span beams and bridges all over the world [1-3]. These girders are consisting of a corrugated web, which is welded with two flange plates. Generally, trapezoidal and sinusoidal corrugations are used in bridges and buildings. Unlike I- plate girders with a traditional plane web, the web of corrugated web girders does not have a significant contribution in bending resistance. This behavior is called accordion effect [4,5]. Hence, for laterally restrained girders with corrugated web, the ultimate moment capacity can be calculated based on the yielding or local buckling capacity of the flanges. On the other hand, the corrugated web, which increases shear buckling stability of the girder, results in an economical girder by elimination of transverse stiffeners essential for a flat web girder. Furthermore, the significant out-of-plane stiffness of the corrugated web reduces the web thickness compared to flat web [1–5]. Zevallos et al. [6] suggested the use two corrugated web plates with small thickness (similar to that suggested by kim et al [7])

Dole Bridge (a) [8]

Koga-Shi Bridge (b) [9]

Fig. 1. Bridges with Corrugated steel Webs

instead of a single web plate with large thickness to increase the strength to weight ratio of the girder. Additionally, this may facilitate and accelerate the production of these girders by benefiting from the recent enhancement in automatic fabrication technology of the corrugated web girders [6]. Based on the previously mentioned advantages, plate girders with corrugated webs have been used in practical applications as shown in Fig. 1, which shows the Dole bridge and Koga-Shi bridge, respectively [8,9]. The corrugated web girder could buckles in local, global, or interaction between local and global buckling modes). The interaction between the local and global shear buckling stresses was recommended to be used in design [1-4,10]. Lindner and Aschinger [11] were the first to propose a generalized formula for the interactive buckling stress. Many researches had been conducted on composite box girder with steel corrugated web (that consist of two top and bottom concrete flanges and steel corrugated webs) [12-13, 14]. In this paper an experimental and modeling investigations had been conducted to study the behavior of a new composite box girder with steel corrugated web (that consist of steel box girder with corrugated web and top concrete flange). Two composite box girder with trapezoidal steel corrugated webs were fabricated and tested under static loading to determine their ultimate capacity. The commercial general-purpose FE package ABAQUS V6.14 was used in this study. The results from Finite element analysis were verified against the experimental results. Failure modes, ultimate loads and load-mid span deflection curve that obtained from the experimental tests were compared with finite element analyses. The comparisons show that the finite element model can predict the behavior of the composite box girder to an acceptable degree of accuracy.

2. Experimental work

2.1. Fabrication of the tested girders

Two composite box girders with steel corrugated web specimens were fabricated [15]. One of the specimens was designed to be loaded in three-point bending (CBGW1, which has one intermediate diaphragm), while the other was designed to be loaded in four-point bending (CBGW2, which has two intermediate diaphragms). Fig.2 shows the nominal geometry and details of a typical specimen. Nelson studs were used as shear studs to tie the concrete slab to the top steel flanges. The fabrication processes of the specimens are shown in Fig. 3.

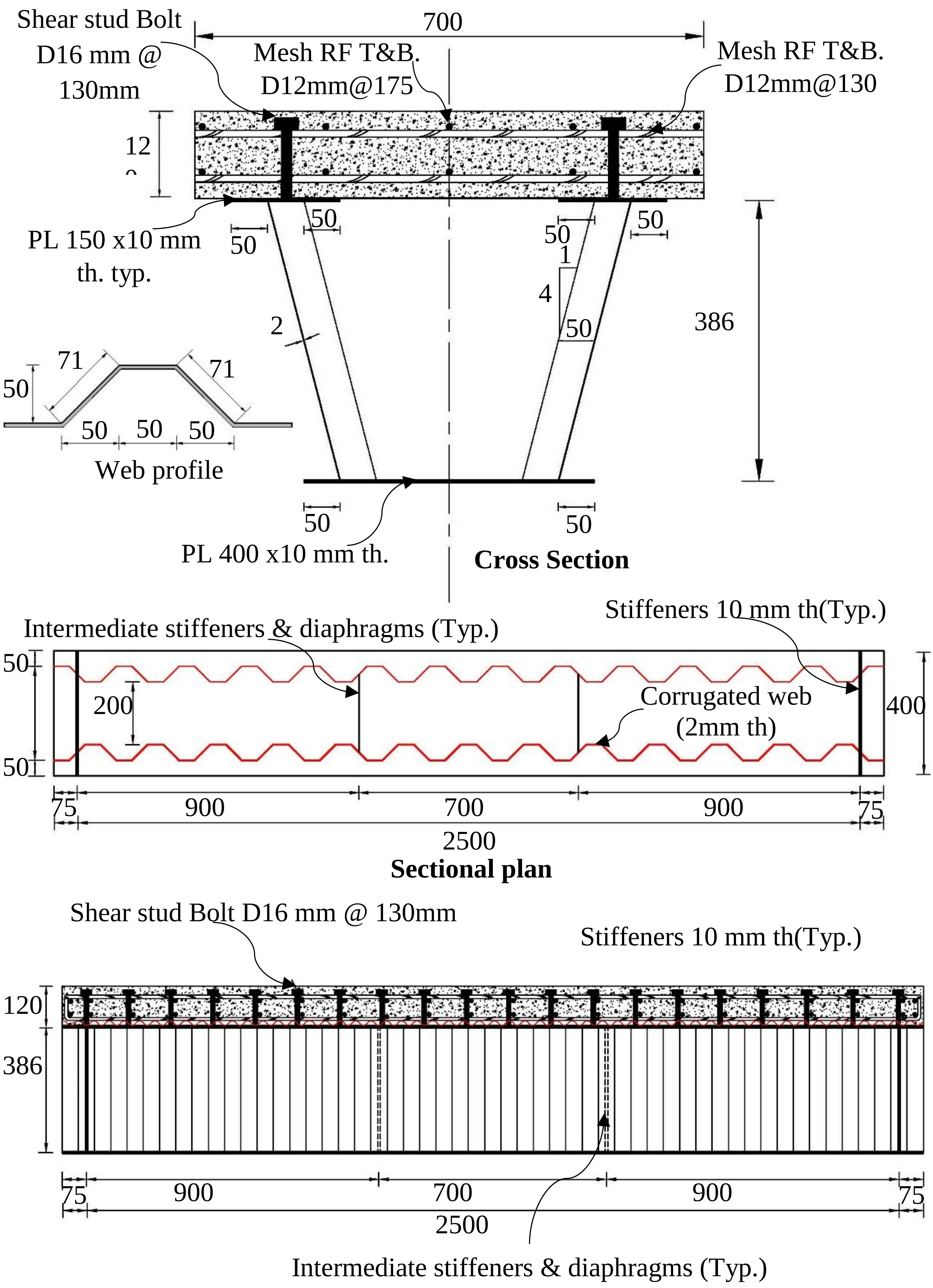

Fig. 2. Nominal geometry of specimens (all dimensions are in mm)

Fig. 3. Specimen fabrication

2.2. Material properties

2.2.1 Concrete

The concrete mix was designed to achieve a compressive strength of 25 N/mm^2 after 28. Six cubes, per each specimen, were tested to determine the actual compressive strength of concrete. The average concrete compressive strength was 27.5 N/mm^2.

2.2.2 Reinforcement steel

Tensile test was performed on a reinforcement bar to determine its mechanical properties. The yield and ultimate strengths were 560 MPa and 670 MPa, respectively.

2.2.3 Structural steel

Six standard tensile coupon specimens (three from the flanges and three from the web as shown in Fig. 4) were cut from the steel specimen plates, prior to fabrication, to determine their mechanical properties. Tables 1 shows the obtained average mechanical properties (yield and ultimate strengths and elongation percentage).

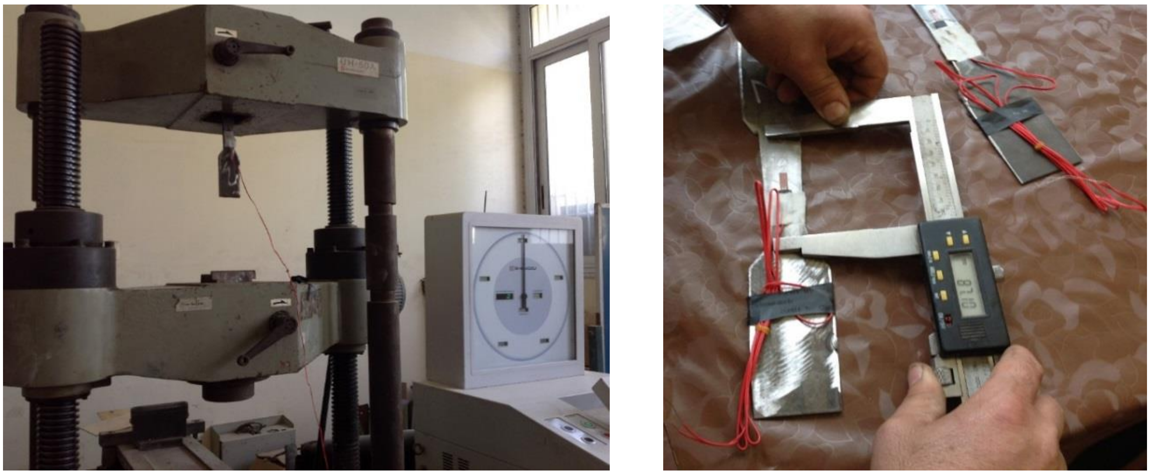

Fig. 4. Tensile coupon specimens

Table 1. Average mechanical properties of steel plates

Type	Yield stress (MPa)	Yield stress (MPa)	Elongation (%)
Flange	418	530	25
Web	405	528	15

2.3. Test setup and loading instrumentations

Fig. 5 shows the typical instrumentations for test specimens CBGW1 and CBGW2. The test specimens were instrumented with a combination of displacement transducers (LVDT) and uniaxial strain gauges. A total of 8 uniaxial strain gauges and 5 LVDTs were used. The test data were acquired and processed using data acquisition system and personal computer. Three strain gauges were installed on both bottom steel and concrete flanges. The remaining strain gauges were located on the corrugated web. Three LVDT was vertically located at the bottom flange to measure the vertical displacement and the others LVDTs were horizontally located at center of concrete slab and top steel flange at one end of specimen to measure slip between the concrete slab and the steel flange. These locations are shown in Fig. 5.

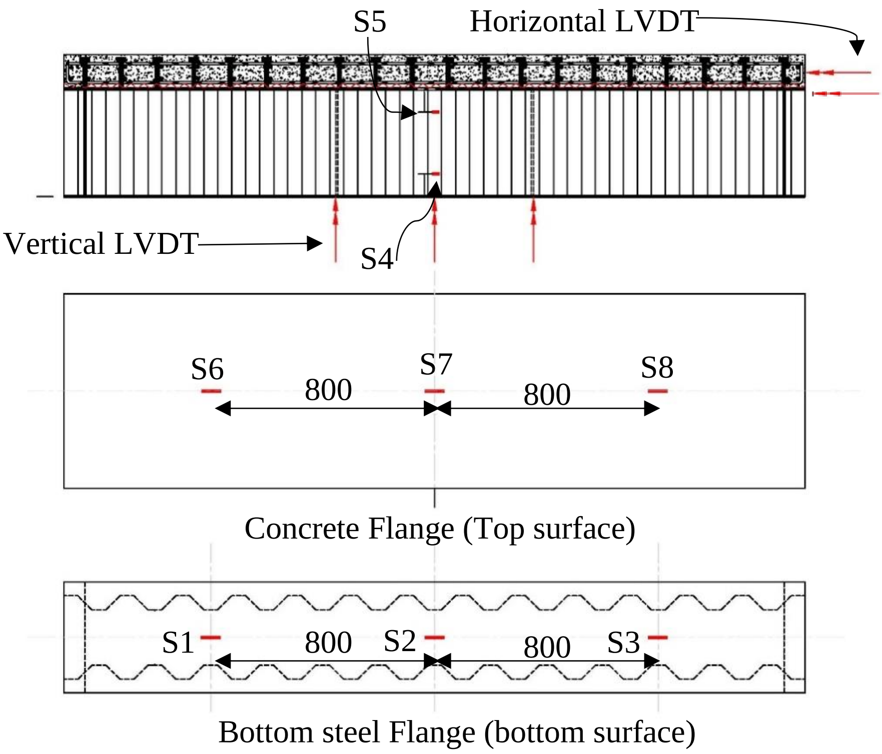

Fig. 5. Instrumentation plan of specimens (all dimensions are in mm)

The tests were performed using a Five-Million-Newton Universal testing machine in National Research Center Laboratory, Cairo, Egypt. The main characteristics of the test setup and fixtures are shown in Fig. 6. The specimen is mounted on a stiffened steel pedestal. The tested girders were placed over the support at their ends, which is in line with the end-bearing stiffeners to avoid local flange and web failure, as shown in Fig. 6. The strain gauges were initialized after ensuring that all instruments were working properly.

Fig. 6. Test setup

2.4. Results and discussion

The two specimens failed in shear failure mechanism and showed similar behavior. Once the shear buckling strength of corrugated web is achieved, the web buckled. The buckling of the web was followed by appearance of shear cracks in concrete flange at buckled web panel. Then, the buckle wave extended to top and bottom steel flanges with inclination of approximately 45°. The buckled wave appeared in the two corrugated webs for tested specimens. Due to buckling of web, a tension field zone was development at the buckled panel and plastic hinges were formed in steel flanges. Then, fracture in webs and concrete crushing were occurred as shown in Fig. 7.

2.4.1 Load–deflection relationship and failure mode

The relationship between load and mid-span deflection for specimens CBGW1, CBGW2 are represented in Fig. 8 (a) and (b), respectively. The ultimate load was 835 kN for CBGW1 and 1055 kN for CBGW2 which are corresponding to 11mm and 9 mm deflection, respectively. For the two specimens, the failure was controlled by shear web buckling. The buckling occurred at the nearest three folds to the support for the two specimens. Although, there are differences between the two specimens in loading condition, both specimens failed at similar locations. The moment shear interaction does not have a significant effect on the shear failure of tested specimens. From Fig. 8, it can be seen that, the load mid-span deflection curve can be divided into two main stages. The first stage is linear, where the deflection is linear until the web starts to buckle. Once the web buckled, a tension field action was developed (second stage) and the post-buckling started. In this stage, the load slightly increases with significant increase in deflection. Unlike the bare steel with corrugated web, composite box girder with steel corrugated web behaves in a reasonably ductile manner. The developed tension field action in the corrugated web is clearly shown in Fig. 7. As soon as the corrugated web buckled in shear, it lost its resistance to carry additional compressive stresses. In this post-buckling stage, a new load-carrying mechanism is developed, where the additional shear load is carried by inclined tensile membrane stress field. The tension field force is anchored in top and bottom steel flanges. The formed plastic hinges are significantly affected by the flexural stiffness of the steel flanges. The composite action between the compression top steel flanges and concrete flange (that is achieved by shear studs) of the girder increases its flexural stiffness and hence a reasonable ductile behavior is achieved.

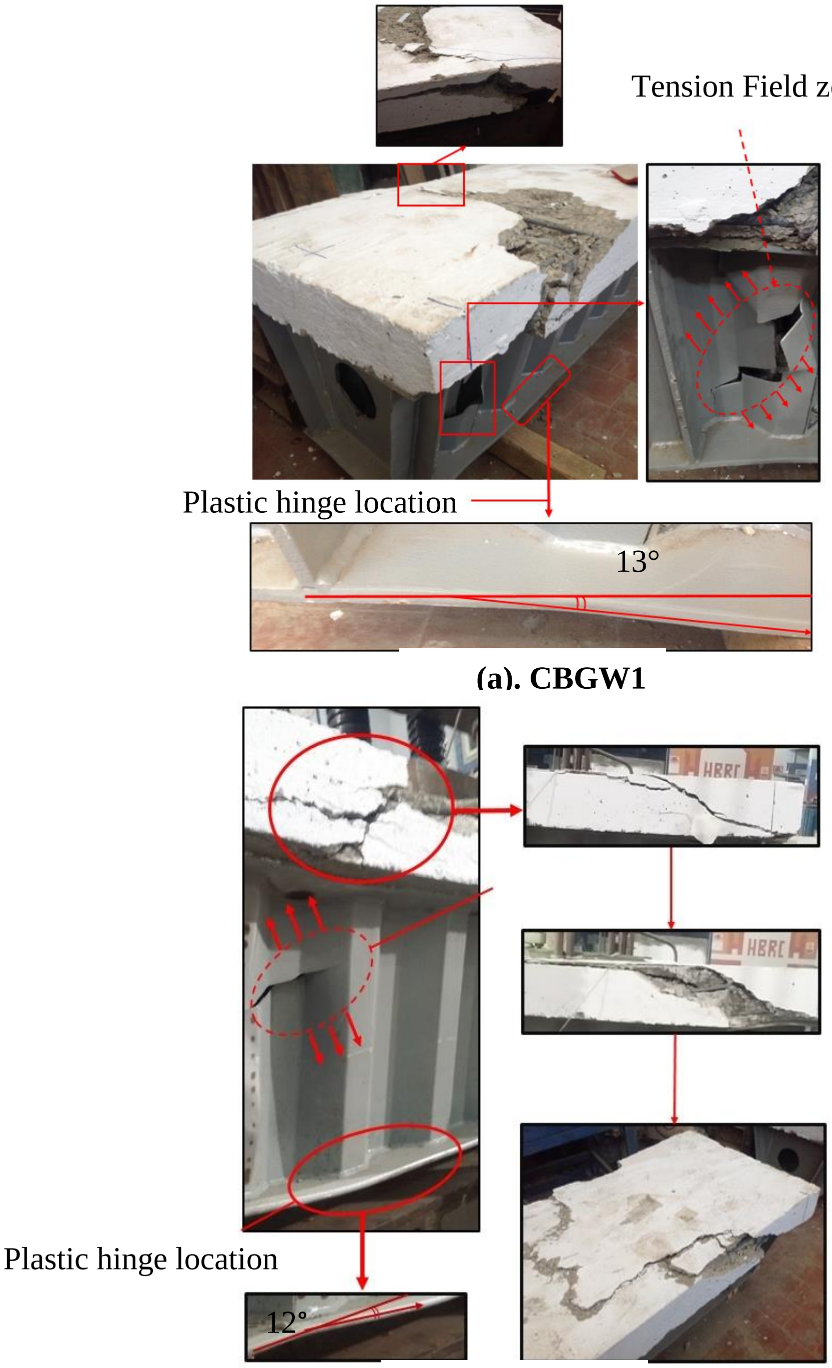

(a). CBGW1

(b). CBGW2

Fig. 7. Tested specimens after failure

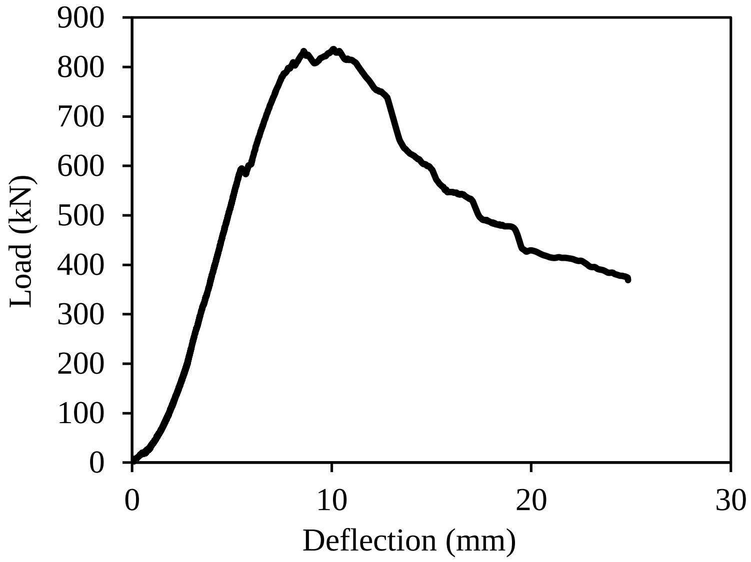

a. Load versus mid-span deflection for specimen CBGW1

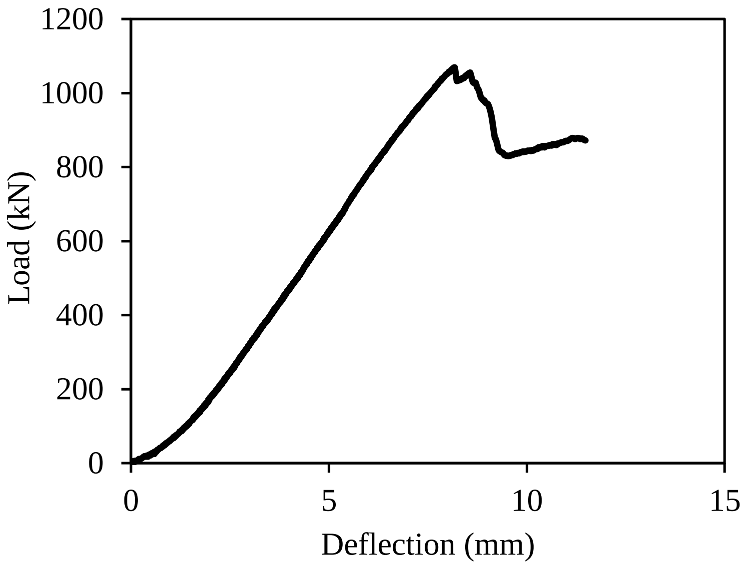

b. Load versus mid-span deflection for specimen CBGW2

Fig. 8. Load versus mid-span deflection for specimens CBGW1,CBGW2

2.4.2 Strain Results

The load versus strain at different locations for specimens CBGW1 and CBGW2 is shown in Figs. 9 and 10, respectively. The measured strains were plotted to study the behavior of the tested composite box girder with steel corrugated web. The strains linearly increased with the load in first loading stage. Once the web buckled and the tension field zone is developed, the strains increase rapidly in the failed shear panel side. The strains decrease at opposite side of the failed shear panel. The normal strains were maximum at plastic hinge locations confirming the tension field mechanism.

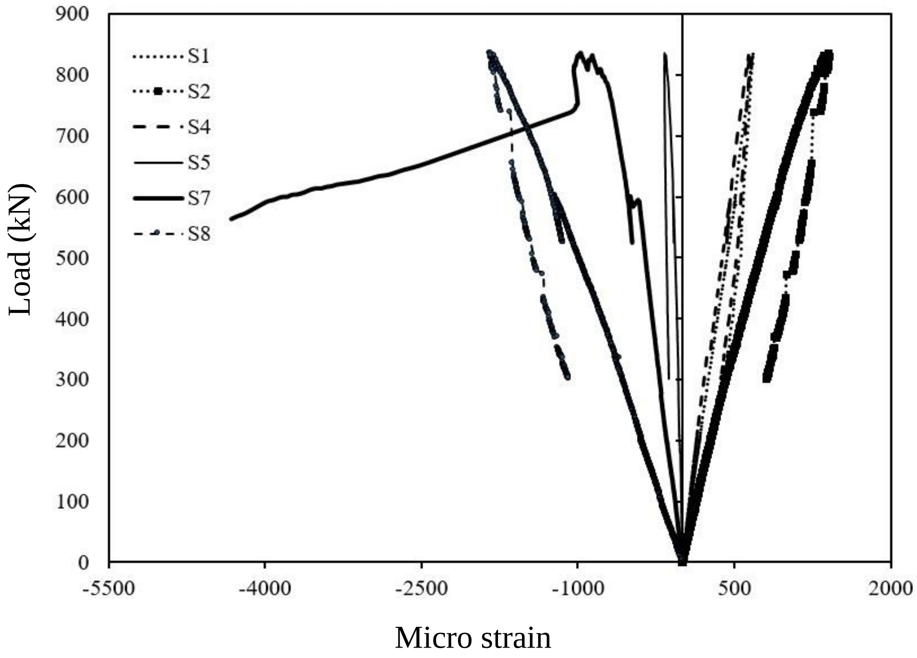

Fig. 9. Load-strain curves for specimen CBGW1

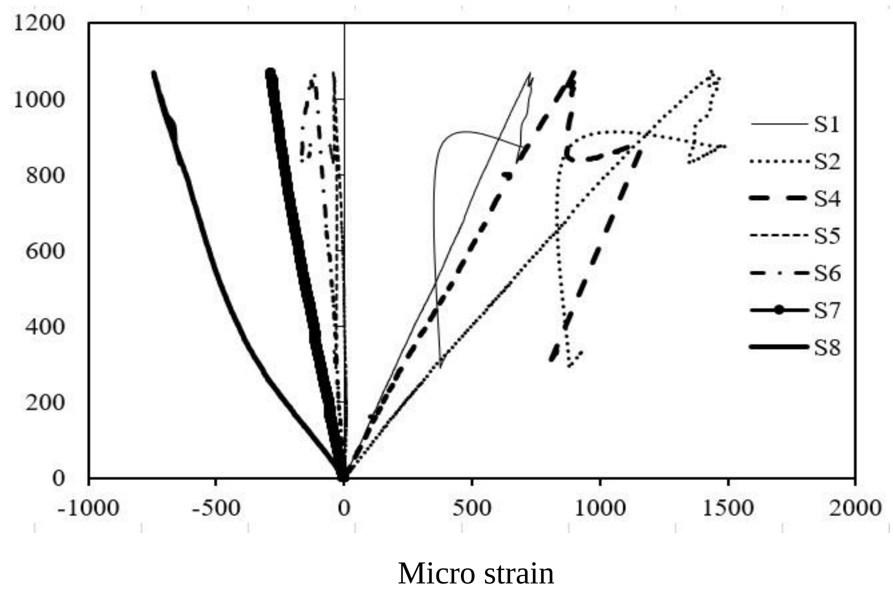

Fig. 10. Load-strain curves for specimen CBGW2

3. Finite Element Modeling

A three-dimensional nonlinear finite element modeling procedure was used to accurately assess the behavior and capacity of steel girder with steel corrugated web. The commercial general-purpose FE package ABAQUS V6.14 is used in this study [16]. ABAQUS 6.14 provides complete material and geometric modeling capabilities with a variety of available element types. A four-node doubly curved shell element with reduced integration (S4R) is used to model the flanges, corrugated web and concrete flange. These elements are suitable for complicated buckling behavior. The S4R element has 6 degrees of freedom per node and provides an accurate solution to most applications. It includes transverse shear deformation, which is important in simulating thick shell elements [16]. Since local and global buckling of corrugated web are very sensitive to large strains, the S4R is used in this study to ensure the accuracy of the results. ABQUS/CAE V6.14 has three different models to simulate the concrete behavior; the smeared cracking models, brittle cracking model and the concrete damaged plasticity model (CDP). Each one of these types is suitable for only certain types of structures and loading conditions. In this study the concrete damaged plasticity was used because it the most comprehensive continuum model that was used in composite slab simulation to define concrete behavior. The shear forces at the steel–concrete flanges interface of tested girders CBGW1, CBGW2 are transformed by the mechanical action of headed stud shear connectors that were detailed in experimental work. Load-slip curve of headed shear studs is very important in modeling the shear interaction between steel flange and concrete slab. Many parameters affect the load-slip characteristics of headed stud such as strength of concrete, diameter of studs, height of stud and strength of stud. The load-slip curve for headed shear studs was inserted in the Finite element model using nonlinear spring in horizontal direction at the location of the shear studs. Another vertical rigid spring with high stiffness was located at the shear stud to transfer the vertical pressure between concrete slab and steel flanges. The typical finite element model is shown in Figure 11.

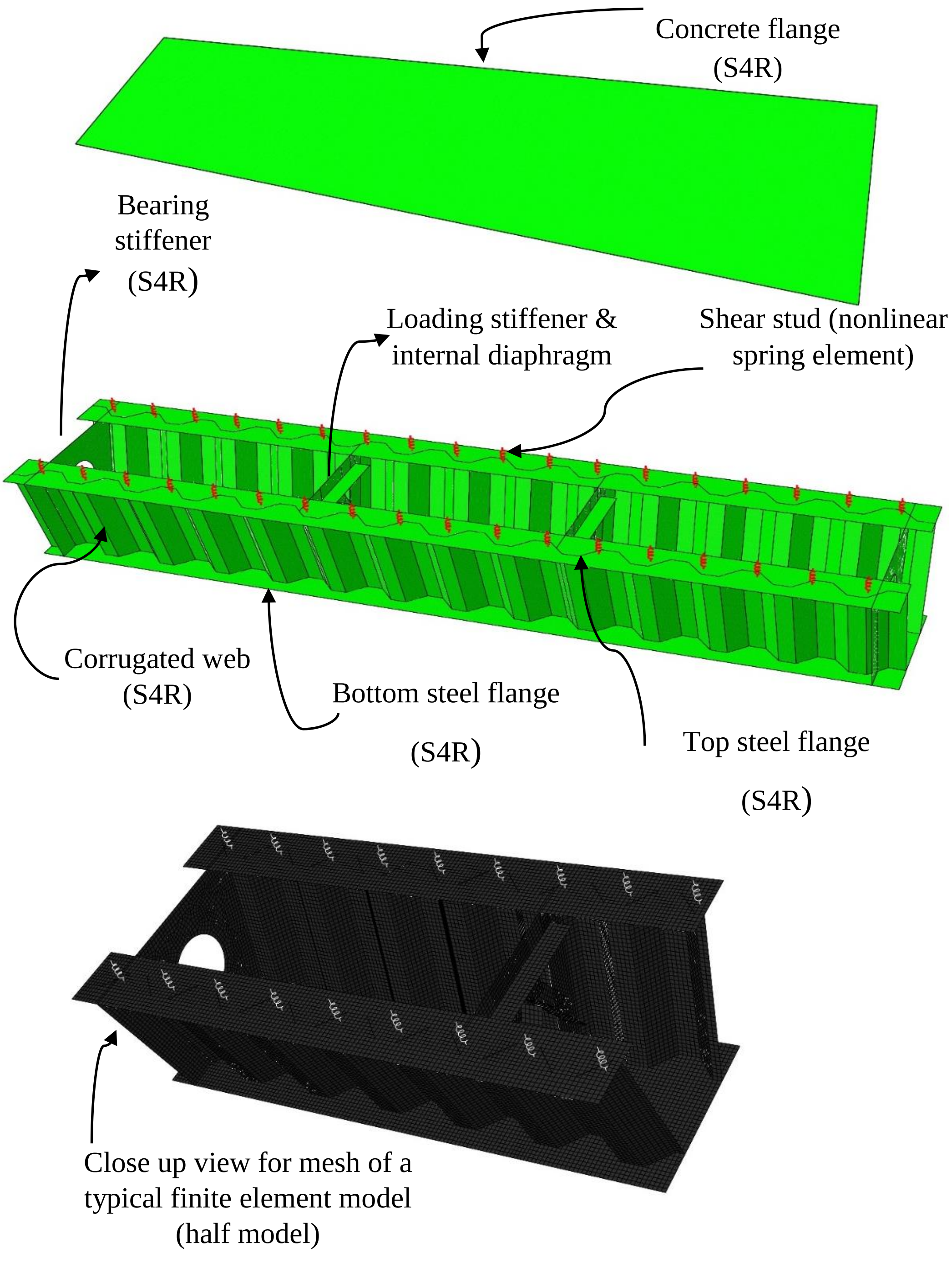

Fig. 11. Typical finite element model for tested specimens

3.1 Results and discussions

The developed finite element models for specimens CBGW1 and CBGW2 were verified using the experimental results. The load-mid span deflection and failure modes that were obtained from experimental tests were compared with finite element results. As shown in Figs. 12 and 13, the Finite element results agree well with experimental results.

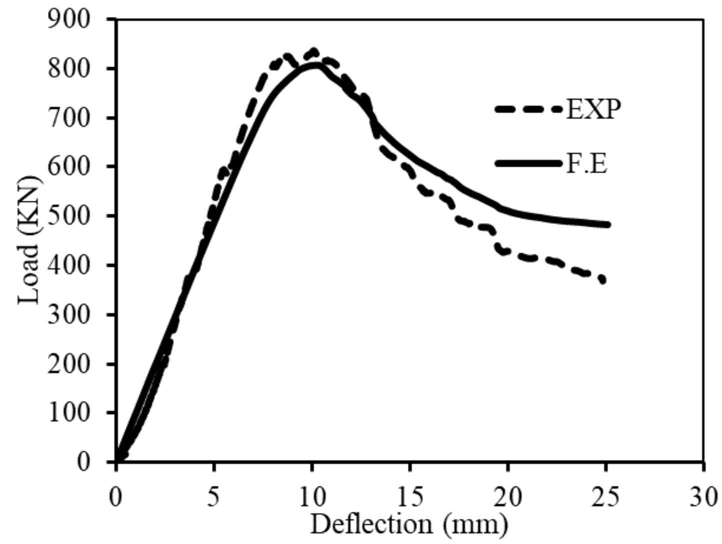

Fig. 12. Load-mid span deflection curve (CBGW1)

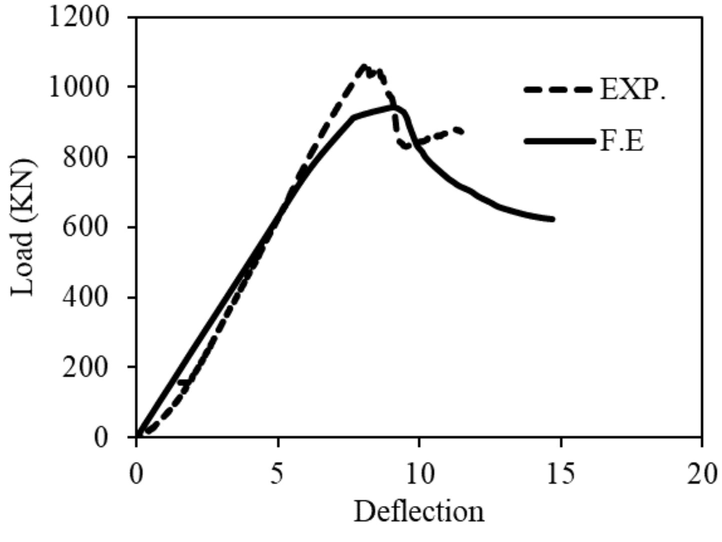

Fig. 13. Load-mid span deflection curve (CBGW2)

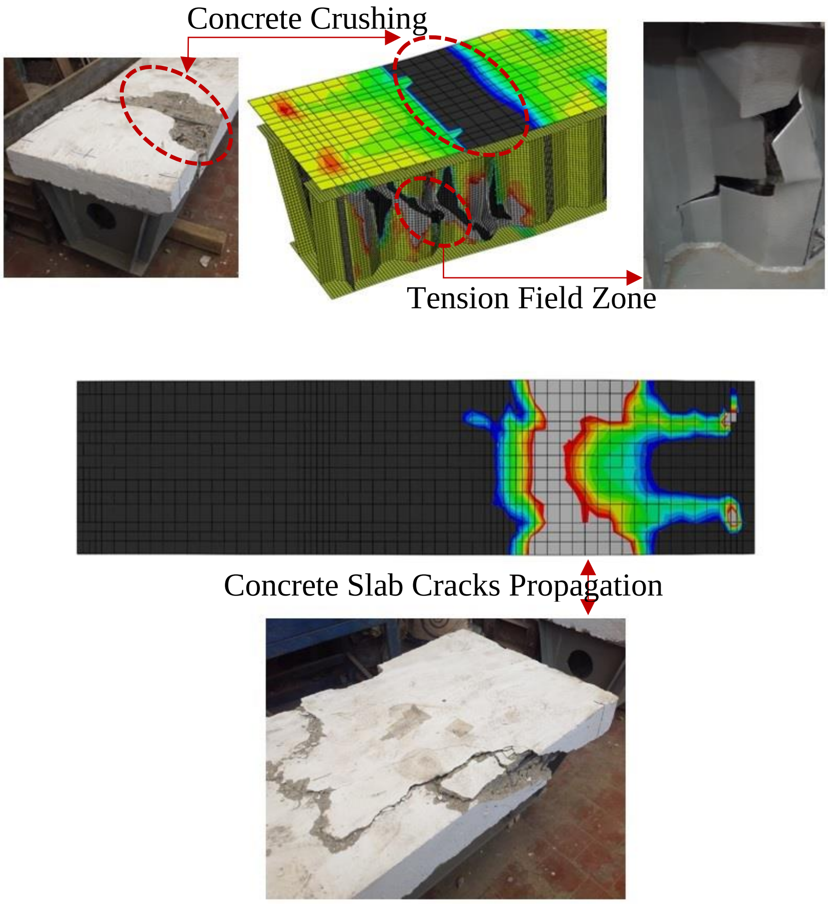

Fig. 14. Experimental and predicted failure modes

The finite element analysis was able to predict the maximum load which was 806 kN for specimen CBGW1 and 942 kN for specimen CBGW2. The maximum experimental load was 835 kN for specimen CBGW1 and 1055 kN for specimen CBGW2. The concrete slab crack propagation and concrete crushing that predicted from the finite element model and observed from the experimental test are shown in Fig. 14. The matching crack pattern from finite element models and experimental specimens is clearly shown.

A tension field zone was developed once the web was yielded. The tension field force in the yielded zone of the web is anchored in the bottom and top flanges. The presence of concrete flange results in a stiffer top steel flange. Moreover, the shear studs act as anchors for top steel flange that bent inward due to the tension field action. It can be seen from Fig. 14 that the cracks are concentrated at shear stud locations and are limited with the top steel flange width, then the cracks propagated across the total width of concrete slab.

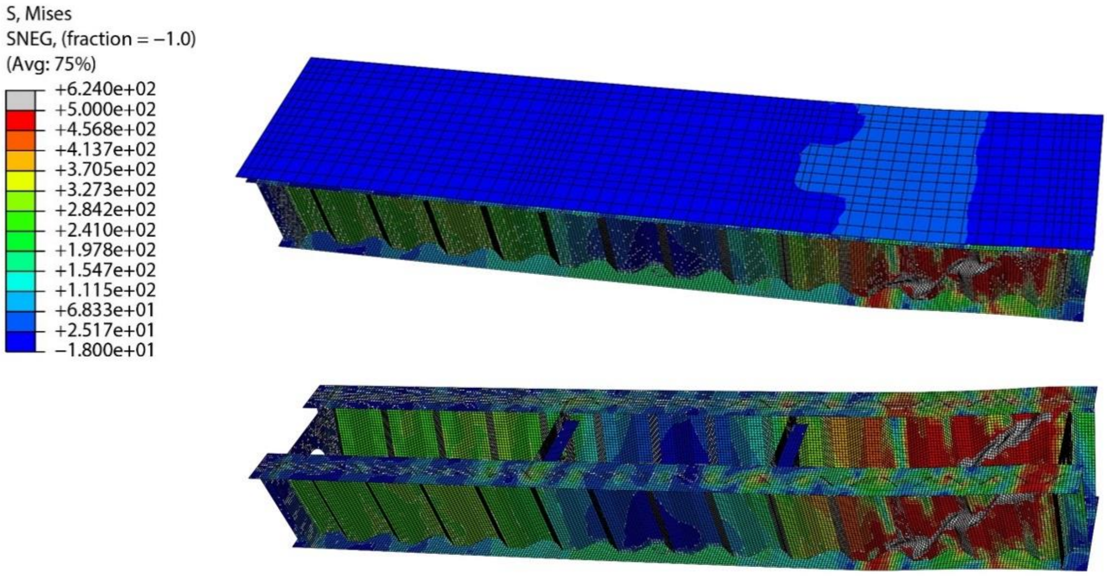

Fig. 15. Von Mises stresses (CBGW2)

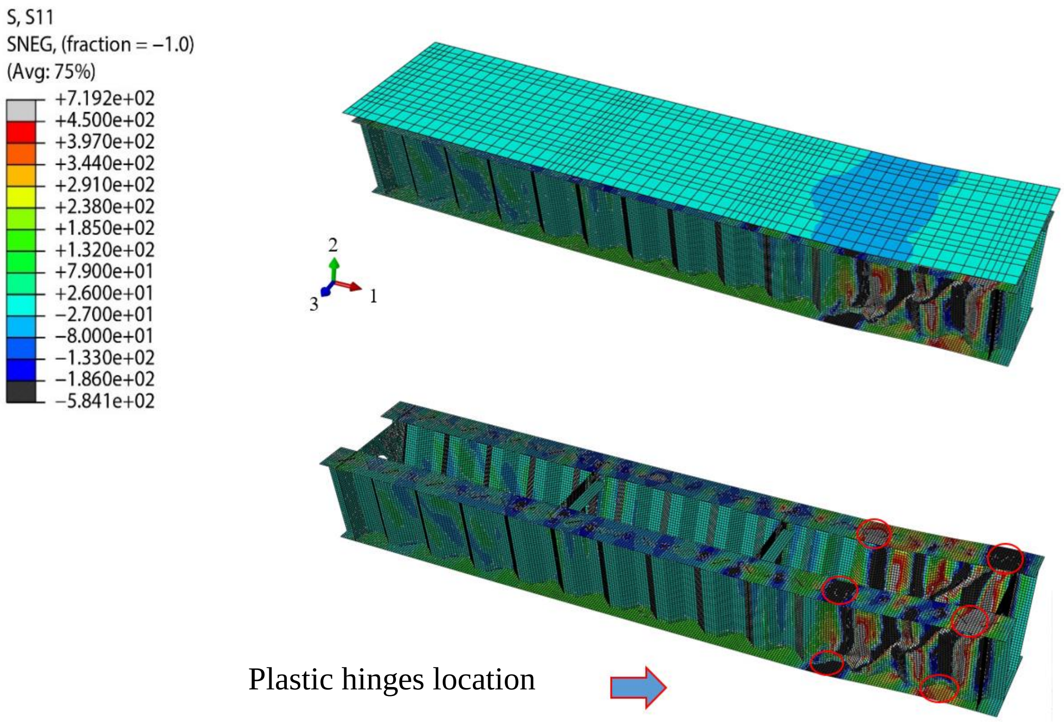

Fig. 16. Normal stresses at failure (CBGW2)

This indicates that the effective width for shear resistance of concrete slab is conservatively equal to the top steel flange width. The von Mises stress contours at failure of specimen CBGW2 are plotted in Fig. 15. It can be seen that, the stresses are concentrated in top and bottom flanges at plastic hinge locations and web yielded zone. Furthermore, the normal stress contours at failure of specimen CBGW2 is shown in Fig. 16. Similarly, the normal stresses are concentrated with high values at the plastic hinge locations in top and bottom flanges.

4. Conclusions

In this study, an experimental and finite element analysis of composite box girders with corrugated steel web were performed to investigate their shear behavior. The following conclusions are drawn from this study:

1. The composite box girders with steel corrugated webs behave in a reasonably ductile manner.
2. An additional shear strength of corrugated steel web is developed after web buckling. This additional shear strength is resisted by tension field mechanism.
3. The concrete slab contributes in enhancing the shear behavior of steel box girder with corrugated web by preventing the anticipated sudden failure of the corrugated web.

4. References

1. Yi, J., Gil, H., Youm, K., & Lee, H. (2008). Interactive shear buckling behavior of trapezoidal corrugated steel webs. *Engineering Structures*, *30*(6), 1659-1666.
2. Moon, J., Yi, J., Choi, B. H., & Lee, H. E. (2009). Shear strength and design of trapezoidal corrugated steel webs. *Journal of Constructional Steel Research*, *65*(5), 1198-1205.
3. Eldib, M. H. (2009). Shear buckling strength and design of curved corrugated steel webs for bridges. *Journal of Constructional Steel Research*, *65*(12), 2129-2139.
4. Hamilton, R. W. (1993). *Behavior of welded girders with corrugated webs* (Doctoral dissertation, in Civil Engineering, University of Maine).
5. Driver, R. G., Abbas, H. H., & Sause, R. (2006). Shear behavior of corrugated web bridge girders. *Journal of Structural Engineering*, *132*(2), 195-203.
6. Zevallos, E., Hassanein, M. F., Real, E., & Mirambell, E. (2016). Shear evaluation of tapered bridge girder panels with steel corrugated webs near the supports of continuous bridges. *Engineering Structures*, *113*, 149-159..
7. Kim, K. S., Lee, D. H., Choi, S. M., Choi, Y. H., & Jung, S. H. (2011). Flexural behavior of prestressed composite beams with corrugated web: Part I. Development and analysis. *Composites Part B: Engineering*, *42*(6), 1603-1616.
8. http://www.hera.org.nz/Story?Action=View&Story_id=1295; 2013.
9. http://www.psmic.co.jp/works/technology/g_jyoubu_d/000100.html, 2007
10. Sause, R., & Braxtan, T. N. (2011). Shear strength of trapezoidal corrugated steel webs. *Journal of Constructional Steel Research*, *67*(2), 223-236.
11. Lindner, J. (1988). Granzschubtragfahigkeit von I-Tragern mit trapezforming profilierten Stegen. *Stahlbau*, *57*, 377-380.
12. Ikeda, S., & Sakurada, M. (2005, August). Development of Hybrid Prestressed Concrete Bridges with Corrugated Steel Web Plates. In *30th Conference on Our World in Concrete & Structures, Singapore* (pp. 23-24).
13. Mizuguchi, K., Ashizuka, K., Furuta, K., Ohura, T., Taki, K., & Kato, T. (1998). Design and construction of the Hondani Bridge: PC bridge using corrugated steel webs. *Bridge and Foundation*, 2-9.
14. Mizuguchi, A., Yoda, S., & Sakurada, H. (1998). Loading tests of Hondani Bridge-PC Bridge Using Corrugated Steel Webs Cantilevering Construction Method. *Bridge and Foundation*, *32*(10), 25-34.
15. Mahmoud, A.M, Behavior of composite box girder with steel corrugated webs. Ph.D. thesis, Al-Azhar University, Faculty of Engineering, Civil Engineering Department 2018, under revision.
16. ABAQUS Standard User's Manual. The Abaqus Software is a product of Dassault Systems Simulia Corp., Providence, RI, USA Dassault Systems, Version 6.14, USA; 2014.